

Signature of a universal statistical description for drift-wave plasma turbulence

Johan Anderson and Pavlos Xanthopoulos

Max-Planck-Institut für Plasmaphysik, IPP-Euratom Association, Teilinstitut Greifswald, D-17491 Greifswald, Germany

(Received 24 August 2010; accepted 6 October 2010; published online 2 November 2010)

This letter provides a theoretical interpretation of numerically generated probability density functions (PDFs) of intermittent plasma transport events. Specifically, nonlinear gyrokinetic simulations of ion-temperature-gradient turbulence produce the time series of heat flux that manifestly exhibit non-Gaussian PDFs with enhanced tails. It is demonstrated that, after the removal of autocorrelations, the numerical PDFs can be matched with predictions from a fluid theoretical setup based on the instanton method. This result points to a universality in the modeling of intermittent stochastic process offering a predictive capability. © 2010 American Institute of Physics. [doi:10.1063/1.3505824]

Stochastic physical processes are most often observed to be unimodal with exponential tails,¹ a feature that is also attributed to fluctuations in magnetically confined plasmas.^{2–7} These fluctuations are intermittent events manifesting a patchy spatial and bursty temporal structure, pertaining to radially propagating coherent structures such as blobs or avaloids,⁸ and have been suggested to carry a significant fraction of the total transport.⁹ Therefore, a comprehensive predictive theory is called for in order to understand and subsequently improve the properties related to intermittency. A major goal would be, for instance, the control of edge heat flux loads, which depend on the instant amplitude of fluctuations, as opposed to the mean load, which can be calculated by quasilinear theory.

In terms of a mathematical description, the likelihood of intermittent events related to plasma turbulence is expressed by probability density functions (PDFs), which usually deviate significantly from the Gaussian distribution. Along these lines, there have been attempts to characterize the statistical properties of the PDFs based on phenomenological premises^{10,11} or numerical investigations^{12,13} alone. Here, however, we carry out a direct comparison between first-principles analytical modeling and numerical simulations. As will be evident in the sequel, although the two approaches express the same physics, they nevertheless greatly differ in their theoretical backgrounds. A key finding of this work is that the intermittent process in the context of drift-wave turbulence appears to be independent of the specific modeling framework, opening the way to the prediction of its salient features.

The main part of this letter consists in providing a theoretical interpretation of the PDFs of radial heat flux derived by nonlinear, local, gyrokinetic simulations of drift-wave turbulence in tokamaks. Our paradigm in this work is the ion-temperature-gradient (ITG) turbulence with adiabatic electrons.¹⁴ The simulations have been carried out with the GENE code¹⁵ in a simple large aspect ratio, circular tokamak geometry. In particular, we calculate the turbulent ion radial heat flux, $Q = \langle v_r \int (\frac{1}{2} m_i v_{\parallel}^2 + \mu B) F_i dv^3 \rangle$, where v_r is the radial

$E \times B$ velocity, v_{\parallel} is the parallel velocity, μ is the magnetic moment, m_i is the ion mass, F_i is the perturbed ion gyrocenter distribution function, and B is the modulus of the magnetic field. The brackets denote spatial averaging over the entire simulation domain. In order to perform a reliable comparison, we produce a series of different cases by varying the magnetic shear $\hat{s} = (r/q)(dq/dr)$ (q is the safety factor, i.e., the number of toroidal turns of the magnetic field for each poloidal turn), which appears both in the gyrokinetic simulations and the theoretical model. There is nothing special about the selection of this parameter, and a similar scan could be performed over, for example, the ion temperature or density gradient. Here, we have set the (normalized) ion-temperature gradient $R/L_{T_i} = 9$, the density gradient $R/L_n = 2$, and the ion-to-electron temperature ratio $\tau = 1$.

For each case, the time evolution of the ion heat flux is considered as a time series to which we apply the standard Box–Jenkins modeling.¹⁶ This mathematical procedure effectively removes deterministic autocorrelations from the system, allowing for the statistical interpretation of the residual part, which *a posteriori* turns out to be relevant for comparison with the analytical theory. In our setup, it turns out that an ARIMA(3,1,0) model accurately describes the stochastic procedure, in that, one can express the (differenced) heat flux time trace in the form

$$Q_{t+1} = a_1 Q_t + a_2 Q_{t-1} + a_3 Q_{t-2} + Q_{res}(t), \quad (1)$$

where the fitted coefficients a_1, a_2, a_3 describe the deterministic component and $Q_{res}(t)$ is the residual part (noise). The reliability of the produced autoregressive model was routinely verified via portmanteau testing and overfitting.

It is systematically observed that the residual PDFs are manifestly non-Gaussian with elevated tails, as shown for instance in Fig. 1, for the case $\hat{s} = 1.0$, where the sample residuals from a GENE simulation are tested against the Gaussian distribution, via a normal quantile-quantile plot. Furthermore, two significant statistical quantities, namely, the variance $\sigma^2 = \langle Q^2 \rangle - \langle Q \rangle^2$ and the kurtosis $K = \langle Q^4 \rangle / \sigma^4$ (here, the brackets denote averaging over the statistical

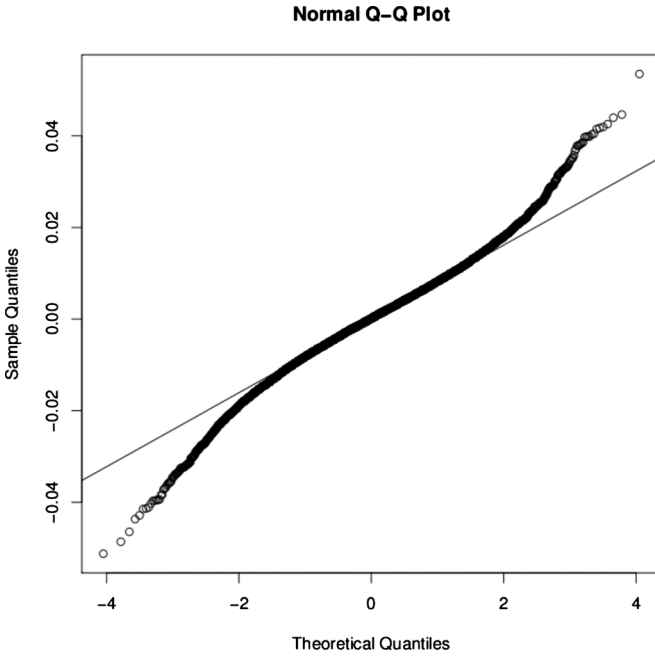


FIG. 1. Normal quantile-quantile plot showing a strong deviation of the residual PDF from Gaussian statistics, in view of the enhanced tails, representing about half of the sample.

sample), during the magnetic shear scan are summarized in Table I. Evidently, the decrease of the variance and the rapid increase in kurtosis for increasing magnetic shear renders a Gaussian description improper. We note in passing that the values of \hat{s} were selected such that the resolution of the simulation domain remains constant, thus avoiding numerical artifacts.

In the sequel, it will be shown that the aforementioned PDF tails can be satisfactorily predicted, starting from a fluid model consisting of a continuity and an energy equation,¹⁷ and using a nonperturbative statistical technique, called the instanton method, which has been adopted from the quantum field theory and then modified to classical statistical physics for Burgers turbulence and in the passive scalar model of Kraichnan.¹⁸ In this context, the key element is to identify the bursty or intermittent event with the appearance of a coherent structure (e.g., streamer).

In the following paragraph, we briefly outline the implementation of the instanton method. For more details, the reader is referred to the existing literature.^{19–23} The PDF tail is first formally expressed in terms of a path integral by utilizing the Gaussian statistics of the forcing in the continu-

ity equation in a similar spirit as in Ref. 9. An optimum path will then be associated with the creation of a modon (among all possible paths or functional values) and the action (S_λ , below) is evaluated using the saddle-point method on the effective action in the limit $\lambda \rightarrow \infty$. The instanton is localized in time existing during the formation of the modon. The saddle-point solution of the dynamical variable $\phi(\vec{x}, t)$ of the form $\phi(\vec{x}, t) = F(t)\psi(\vec{x})$ is called an instanton if $F(t) = 0$ at $t = -\infty$ and $F(t) \neq 0$ at $t = 0$. Note that, the function $\psi(\vec{x})$ here represents the spatial form of the coherent structure. Thus, the intermittent character of the transport consisting of bursty events can be described by the creation of modons. The probability density function of the heat flux Q can be defined as

$$P(Q) = \langle \delta(v_r n T_i(\vec{r} = \vec{x}_0) - Q) \rangle = \int d\lambda e^{i\lambda Q} I_\lambda, \quad (2)$$

where

$$I_\lambda = \langle \exp[-i\lambda v_r n T_i(\vec{x} = \vec{x}_0)] \rangle. \quad (3)$$

Here, v_r is the radial drift velocity and T_i is the ion temperature. The integrand can then be rewritten in the form of a path integral as

$$I_\lambda = \int \mathcal{D}\phi \mathcal{D}\bar{\phi} e^{-S_\lambda}. \quad (4)$$

Although $\bar{\phi}$ appears to be simply a convenient mathematical tool, it does have a useful physical meaning that should be noted; it arises from the uncertainty in the value of ϕ due to the stochastic forcing. That is, the dynamical system with a stochastic forcing should be extended to a larger space involving this conjugate variable, whereby ϕ and $\bar{\phi}$ constitute an uncertainty relation. Furthermore, $\bar{\phi}$ acts as a mediator between the observables (heat flux) and instantons (physical variables) through stochastic forcing. In Eq. (4), the integral in λ is computed using the saddle-point method where it is shown that the limit $\lambda \rightarrow \infty$ corresponds to $Q \rightarrow \infty$, representing the tail part of the distribution. Based on the assumption that the total PDF can be characterized by an exponential form, the expression

$$P(Q) = \frac{1}{Nb} \exp\{-b|Q - \bar{Q}|^{3/2}\}, \quad (5)$$

$$b = b_0 \left[\frac{R}{L_n} + 2\langle g_i \rangle \beta - U - \langle k_\perp^2 \rangle \left(U + \frac{R}{L_n} \right) \right], \quad (6)$$

$$\beta = 2 + \frac{2}{3} \frac{R/L_n - U}{U + 10/3 \tau \langle g_i \rangle}. \quad (7)$$

is found²³ where the heat flux Q plays the role of the stochastic variable with $P(Q)$ determining its statistical properties. Several auxiliary definitions are also utilized: the normalization constant N ; the gradient scale lengths $L_f = -(d \ln f / dr)^{-1}$; the normalized modon speed $\tilde{U} = RU/L_n = R/L_n$; and temperature ratio $\tau = T_i/T_e$; $g_i = \omega_d / \omega_\star = (2L_n/R) \times [\cos(\xi) + \hat{s}\xi \sin(\xi)]$ where ω_d is the curvature drift frequency and ω_\star is the diamagnetic drift frequency; $k_\perp^2 = k_y^2(1$

TABLE I. Simulation results.

\hat{s}	Variance	Kurtosis
0.25	5.962×10^{-4}	3.529
0.40	5.253×10^{-4}	3.517
0.50	6.049×10^{-4}	3.527
0.60	5.874×10^{-4}	3.715
0.75	4.403×10^{-4}	4.324
1.00	8.253×10^{-5}	14.413

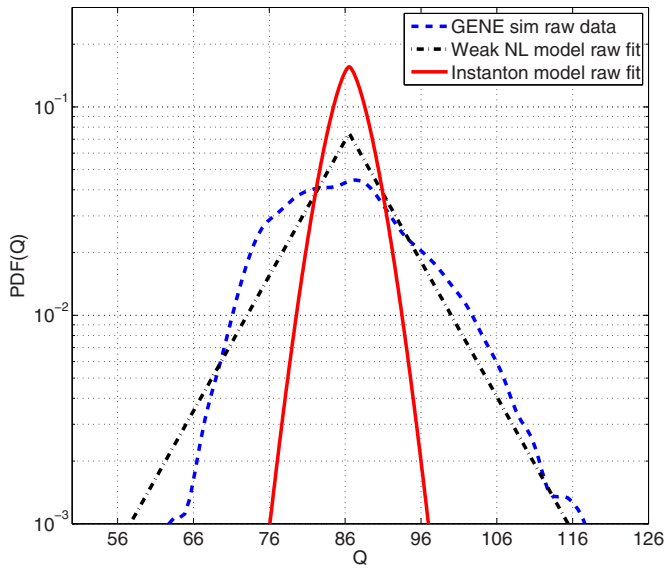


FIG. 2. (Color online) The numerically estimated PDF of heat flux (dashed blue line) in comparison with the analytically predicted instanton method (solid red line) and the weak nonlinear model (dashed-dotted black line) at magnetic shear $\hat{s}=0.25$.

$+\hat{s}^2\xi^2$) is the perpendicular wave number; the brackets denote averaging along the field line, e.g., for an arbitrary scalar function f , $\langle f \rangle = \int_{-\pi}^{\pi} d\xi \phi f \phi / \int_{-\pi}^{\pi} d\xi \phi^2$ where the eigenfunctions $\phi(\xi)$ are extracted from the GENE simulations and \bar{Q} is the mean value of the heat flux. The coefficient b_0 is a free parameter and represents the strength of the forcing in the continuity equation. Note that the proposed PDF is close enough to a Gaussian distribution to match the bulk of the PDF while retaining the enhanced tails. Furthermore, the exponential form of the PDF will be the same for momentum flux with a modified coefficient b , which is in agreement with findings in recent experiments.²⁴

In Fig. 2 ($\hat{s}=0.25$), the PDF of heat flux Q (i.e., stemming from the *raw* timetrace of the simulation) (dashed blue line) is shown. Although a simple visual inspection precludes the Gaussian distribution, the analytically predicted instanton method from Eq. (5) (solid red line) does a rather poor job modeling the simulation result. This is, however, contrasted to the PDF using the weak nonlinear model (dashed-dotted black line) where reasonably good agreement is found similar to what has been reported earlier.^{6,9} Note that all PDFs shown are normalized such that the total probability is unity. The weak nonlinear model (a Laplace distribution) has the form $P(Q) = e^{-|Q-\mu|/b} / (2b)$ where b is determined by the variance. It is important to stress, however, that it can be predicted by the instanton model only when the nonlinearities are neglected.²⁵ The Laplace distribution can be easily obtained by assuming that the background fluctuating fields (i.e., the potential and temperature) are close to Gaussian distributions whereas the resulting distribution for the heat flux is non-Gaussian with an unknown correlation factor. This fact points to the possibility that the total PDF does not reliably represent the statistics of the intermittent process. Along these lines, the well-studied kurtosis-skewness scaling based on the total PDF does not prove to be insightful.²⁶

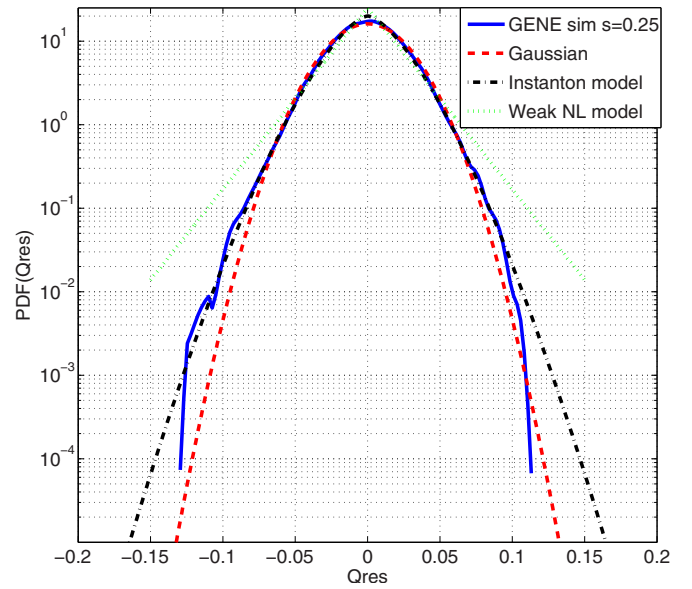


FIG. 3. (Color online) Comparison of the numerically estimated PDF (solid blue line) against the analytically predicted instanton model (dashed-dotted black line) and weak nonlinear model (dashed green line) compared to the best fit Gaussian (dashed red line) for $\hat{s}=0.25$.

Figures 3 and 4 single out the comparison of the numerically estimated residual PDFs against the instanton prediction in Fig. 1. Here, the PDF of Q_{res} from the simulation (blue line) and the analytically predicted PDF from the instanton method (dashed-dotted black line) demonstrate a significantly better agreement both at the tails and the center of the PDF, as compared to the best fit (using the first two moments) Gaussian distribution (dashed red line) at magnetic shears $\hat{s}=0.25$ and $\hat{s}=1.0$, respectively. The coefficient b_0 in Eq. (6) is determined from the simulations at the point $\hat{s}=0.5$ and for the weak nonlinear model a value of the vari-

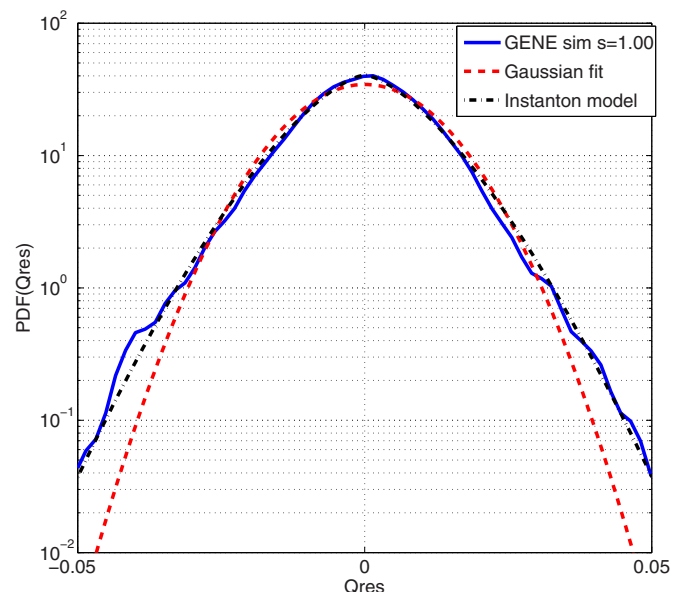


FIG. 4. (Color online) Comparison of the numerically estimated PDF (solid blue line) against the analytical prediction (dashed dotted black line) and the best fit Gaussian (dashed red line) for $\hat{s}=1.0$.

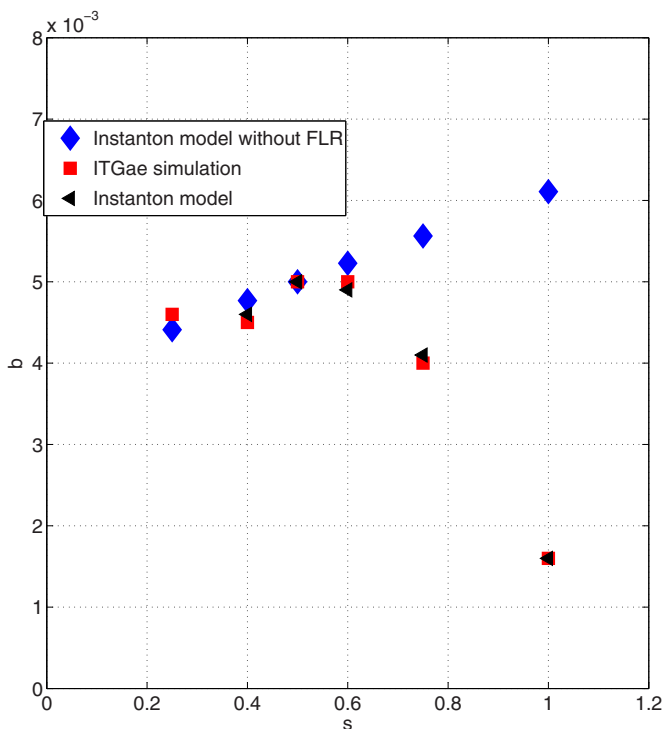


FIG. 5. (Color online) The coefficient b as a function of magnetic shear \hat{s} . The simulation results (red squares) are compared to the analytical fluid model prediction (black stars) and the same with suppressed FLR effects (blue diamonds).

ance of 8.00×10^{-4} was used for better agreement. Note that the weak model does not capture the form of the residual PDF while a surprisingly good agreement is found for the instanton model.

Since the quality of the agreement in the previous figures heavily relies on the exponential coefficient b in Eq. (5), this is displayed for the whole magnetic shear scan in Fig. 5, verifying that good agreement is expected for any value of \hat{s} . Here, we note that the abrupt bending of the curve for larger values of shear is solely attributed to finite Larmor radius (FLR) effects.

In conclusion, we have presented a first quantitative comparison between a first-principles theoretical model of drift-wave turbulence with self-consistent nonlinear simulations. Numerical PDFs of heat flux were generated with the gyrokinetic code GENE in the framework of toroidal ITG turbulence, and subsequently processed with Box–Jenkins modeling in order to remove deterministic autocorrelations, thus retaining their stochastic parts only. These PDFs have been shown to agree very well with analytical predictions based on a fluid model, on applying the instanton method. Specifically, we were able to quantitatively confirm the exponential form of the PDFs, therefore adding the important element of predictive strength to the existing phenomenological approaches. More importantly, a strong indication of universality in the description of drift-wave turbulence has emerged.

In future publications, we will address the emergent universal scalings of the PDFs of potential, density and tem-

perature where the theory predicts different tails.²⁵ A study of potential or density fluctuations opens up opportunities for comparison with experimentally measured PDFs. Still within the scope of ITG turbulence, we will include effects from kinetic electrons, in order to test the robustness of the exponential scaling. A quite interesting complementary work would involve incorporating results from nonlinear fluid simulations, based on Braginskii-like equations, and relate them to the already presented findings. Finally, our present setup provides a testbed for the investigation of the impact of zonal flows on the statistics, as reported elsewhere.¹² The work addressing these avenues has been initiated.

The GENE simulations have been performed at the Jülich Supercomputing Center (JSC). The authors are grateful to Professor P. Helander and Professor F. Jenko for many fruitful discussions.

¹S. T. Bramwell, *Nat. Phys.* **5**, 443 (2009).

²S. Zweben, J. A. Boedo, O. Grulke, C. Hidalgo, B. LaBombard, R. J. Maqueda, P. Scarin, and J. L. Terry, *Plasma Phys. Controlled Fusion* **49**, S1 (2007).

³P. A. Politzer, *Phys. Rev. Lett.* **84**, 1192 (2000).

⁴P. Beyer, S. Benkadda, X. Garbet, and P. H. Diamond, *Phys. Rev. Lett.* **85**, 4892 (2000).

⁵J. F. Drake, P. N. Guzdar, and A. B. Hassam, *Phys. Rev. Lett.* **61**, 2205 (1988).

⁶B. A. Carreras, B. van Milligen, C. Hidalgo, R. Balbin, E. Sanches, I. Garcia-Cortes, M. A. Pedrosa, J. Bleuel, and M. Endler, *Phys. Rev. Lett.* **83**, 3653 (1999).

⁷F. Sattin, P. Scarin, M. Agostini, R. Cavazzana, G. Serianni, M. Spolaore, and N. Vianello, *Plasma Phys. Controlled Fusion* **48**, 1033 (2006).

⁸G. Y. Antar, S. I. Krashenninnikov, P. Devynck, R. P. Doerner, E. M. Hollmann, J. A. Boedo, S. C. Luckhardt, and R. W. Conn, *Phys. Rev. Lett.* **87**, 065001 (2001).

⁹B. A. Carreras, C. Hidalgo, E. Sanches, M. A. Pedrosa, R. Balbin, I. Garcia-Cortes, B. van Milligen, D. E. Newman, and V. E. Lynch, *Phys. Plasmas* **3**, 2664 (1996).

¹⁰I. Sandberg, S. Benkadda, X. Garbet, G. Ropokis, K. Hizandis, and D. del-Castillo-Negrete, *Phys. Rev. Lett.* **103**, 165001 (2009).

¹¹J. A. Krommes, *Phys. Plasmas* **15**, 030703 (2008).

¹²R. Sánchez, D. E. Newman, J.-N. Leboeuf, B. A. Carreras, and V. K. Decyk, *Phys. Plasmas* **16**, 055905 (2009).

¹³G. Dif-Pradalier, P. H. Diamond, V. Grandgirard, Y. Sarazin, J. Abiteboul, X. Garbet, Ph. Ghendrih, A. Strugarek, S. Ku, and C. S. Chang, *Phys. Rev. E* **82**, 025401 (2010).

¹⁴W. Horton, *Rev. Mod. Phys.* **71**, 735 (1999).

¹⁵F. Jenko, W. Dorland, M. Kotschenreuther, and B. N. Rogers, *Phys. Plasmas* **7**, 1904 (2000).

¹⁶G. Box, G. Jenkins, and G. Reinsel, *Time Series Analysis; Forecasting and Control* (Prentice-Hall, Englewood Cliffs, NJ, 1994).

¹⁷J. Anderson, H. Nordman, R. Singh, and J. Weiland, *Phys. Plasmas* **9**, 4500 (2002).

¹⁸E. Balkovsky and V. Lebedev, *Phys. Rev. E* **58**, 5776 (1998).

¹⁹J. Zinn-Justin, *Field Theory and Critical Phenomena* (Clarendon, Oxford, 1989), p. 57.

²⁰V. Gurarie and A. Migdal, *Phys. Rev. E* **54**, 4908 (1996).

²¹G. Falkovich, I. Kolokolov, V. Lebedev, and A. Migdal, *Phys. Rev. E* **54**, 4896 (1996).

²²E. Kim and P. H. Diamond, *Phys. Rev. Lett.* **88**, 225002 (2002).

²³J. Anderson and E. Kim, *Phys. Plasmas* **15**, 082312 (2008).

²⁴Z. Yan, G. R. Tynan, J. H. Yu, C. Holland, S. H. Muller, and M. Xu, *Bull. Am. Phys. Soc.* **52**, 74 (2007).

²⁵E. Kim and J. Anderson, *Phys. Plasmas* **15**, 114506 (2008).

²⁶F. Sattin, M. Agostini, R. Cavazzana, G. Serianni, P. Scarin, and N. Vianello, *Phys. Scr.* **79**, 045006 (2009).